PNAS
www.pnas.org

Supplementary Information for

Dopaminergic neuromodulation of prefrontal cortex activity requires the NMDA receptor co-agonist D-serine

Glenn Dallérac, Xia Li, Pierre Lecouflet, Nadège Morisot, Silvia Sacchi, Rachel Asselot, Thu Ha Pham, Brigitte Potier, David JG Watson, Staffan Schmidt, Grégoire Levasseur, Pascal Fossat, Andrey Besedin, Jean-Michel Rivet, Joseph T Coyle, Ginetta Collo, Loredano Pollegioni, Jan Kehr, Micaela Galante, Kevin C Fone, Alain M Gardier, Thomas Freret, Angelo Contarino, Mark J. Millan, Jean-Pierre Mothet

Jean-Pierre Mothet
Email: jean-pierre.mothet@universite-paris-saclay.fr

Glenn Dallérac
Email: glenn.dallerac@universite-paris-saclay.fr

This PDF file includes:

Supplementary Information Text

Methods and Materials

Animals

For electrophysiology adult male Wistar rats and adult male C57BL/6 $SR^{+/+}$ or $SR^{-/-}$ mice were used. Behavioral experiments were performed on Lister hooded rats purchased from Charles River (UK) and C57BL/6 $SR^{+/+}$ or $SR^{-/-}$ mice. With the exception of Lister hooded rats, animals were bred in-house in polycarbonate cages and maintained on a 12:12-h light/dark cycle in a temperature (22°C) and humidity controlled room. Animals were given access to food and water *ad libitum*.

Electrophysiological recordings

Experiments were carried out as previously described (1). Briefly, acute slices were obtained from 35 to 60 days old rats or mice. Animals were anaesthetized with isoflurane before cervical dislocation and decapitation. The brain was then quickly removed and placed in ice-cold aCSF saturated with 95 % O_2 and 5 % CO_2. Coronal slices (300 µm) containing the medial prefrontal cortex (mPFC) were cut by mean of a vibratome (Leica VT1200S) and allowed to recover for a minimum of 45 min at 30 °C in a submerged chamber containing ACSF before recording. Slices were individually transferred in a recording chamber placed under a microscope (Olympus BX51) and continuously perfused with aCSF (rate:1-2 mL/min) composed of (in mM): NaCl, 123; KCl, 2.5; Na_2HPO_4, 1; $NaHCO_3$, 26.2; $MgCl_2$, 1.3; $CaCl_2$, 2.5; and glucose, 10 (pH 7.4; 295-300 mOsm kg^{-1}).

For patch clamp experiments, pyramidal PFC neurons in layers V/VI of the prelimbic cortex (PrL) were visually identified using infrared differential interference contrast microscopy. Evoked excitatory synaptic currents (EPSCs) were recorded under whole-cell voltage-clamp mode. The patch-clamp recording pipettes (borosilicate glass, Harvard Apparatus, 2.5-5 MΩ) were either filled with a cesium chloride (CsCl) or K-gluconate based solution. The CsCl-based solution contained (in mM): CsCl, 130; NaCl, 10; 4-(2-hydroxyethyl)-1-piperazineethanesulfonic acid (HEPES), 10; QX-314, 5; ethyleneglycol-bis(2-aminoethylether)-N,N,N′,N′-tetra acetic acid (EGTA), 1; and $CaCl_2$, 0.1 (adjusted to pH 7.1–7.3 with CsOH; 292-296 mOsm kg^{-1}). The K-gluconate solution contained (in mM): K-gluconate, 120; KCl, 20; HEPES, 10, EGTA, 1; $MgCl_2$, 1; $CaCl_2$, 0.1 (adjusted to pH 7.1–7.3 with KOH; 292–296 mOsm kg^{-1}). Neurons were first clamped at −70 mV and allowed to dialyze for 10 min before recording. NMDA currents were recorded in the presence of NBQX (10 µM) and picrotoxin (50 µM).

Recording of NMDA receptor currents with the K-gluconate solution were performed at -70 mV in low magnesium aCSF (0.5 mM $MgCl_2$). The CsCl based solution allowed to record NMDA-receptor currents at +40 mV, potential at which the magnesium block is released. Recordings were all performed at 30°C using a Multiclamp 700B amplifier (Axon Instruments, Inc.); signals were filtered at 2 kHz and digitized at 5 kHz *via* a DigiData 1440A interface (Molecular Devices). Series resistance and holding current were monitored throughout experiments. Cells with an access resistance > 25 MΩ at resting potential were excluded from analyses as well as any cell for which a >20 % change in those parameters occurred during the course of the experiment. Stimulation was achieved using a glass electrodes filled with aCSF and placed in layers I/II of the PrL area. Assuming that mean center-to-center distance between minicolumn in the prelimbic area is 45 µm in rats (2), the electrode of stimulation was shifted in order to avoid direct stimulation of the dendritic bundles of the recorded pyramidal neurons. To ensure that the recorded EPSC indeed reflected activation of NMDA receptors, the antagonist D-AP5 was applied. D-AP5 abolished recorded currents at both -70 mV and +40 mV (Fig.1A). NMDA receptor inward currents recorded at -70 mV display a much lower amplitude than outward currents recorded at +40 mV. Small inward and large outward currents were recorded in order to respectively highlight the up- and down-regulation of NMDAR-EPSCs by dopamine. This bidirectional regulation was verified at resting potential (*SI Appendix* Fig. S8).

Recordings of neuronal excitability was performed in the current clamp mode using the K-gluconate based solution and consisted in injecting depolarizing pulse of increasing intensities (0-200 pA; 25 pA increments). Negative current pulses were also applied in order to calculate passive properties; i.e. resting potential, input resistance, membrane time constant and capacitance.

Evoked field potentials were obtained from 400 µm coronal PFC slices. As for patch experiments, the stimulating electrode was placed in layer I/II of the PrL area and the recording electrode consisting in a glass pipette filled with 1 M NaCl in Layer V. input/output relationships were assayed with increasing stimulation (5-30 V, increment 5 V, 40 µs width), at 0.067 Hz. The test shock used in subsequent recordings was chosen to elicit one third of the maximal slope for paired-pulse and long-term potentiation experiments, two third for long-term depression experiments. Paired-pulse experiments consisted of 2 identical stimuli with increasing inter-pulse intervals (50-250 ms, 50 ms increment) delivered at 0.033 Hz. Paired-pulse ratios were generated by plotting the maximum slope of the second response (P2) as a percentage of the first (P1) using the following formula: (P2/P1 x 100) – 100. LTP was induced by high-frequency stimulation (HFS: 6 trains of 100 pulses at 50 Hz, 10 s inter-train interval). LTD was induced by low-frequency stimulation (LFS: 3 Hz, 15 min).

Electrophysiological data were collected and analyzed using pClamp10 software (Axon Instruments, Inc.) or Elphy™ (Biologic UNIC-CNRS, Gif sur Yvette, France). Data are expressed as mean ± SEM. LTP and LTD levels were defined as the percent change in fEPSP slope during the last 30 min of recordings (30-60 min post-HFS). Changes in NMDAR-EPSC amplitudes were assessed during the last 5 min of recording.

Behavioral testing

Novel object recognition (NOR) was assessed in both rats and mice as described previously (3, 4) .The NOR apparatus used for mice was a dark grey polypropylene box (40 x 30 x 23 cm; length, width, height). A glass-made rectangle and a ceramic bowl were used for object recognition; they were about 5 cm high, too heavy to be displaced by the animal and located 5 cm away from a corner of the apparatus. The mice did not show any preference for either of the two objects. For both rats and mice behavioral testing was conducted during the light phase of the 12 h light/dark cycle under dim illumination (30 lux for mice, 100 lux for rats). As described previously (3, 4), prior to the first NOR test, during three consecutive days animals were handled 1 min per day. On the day preceding each NOR test, animals were allowed to freely explore the empty (without object) apparatus for 10 min (mice) or 60 min (rats) during the habituation trial. The NOR test consisted of 2 trials (T1 and T2) separated by an inter-trial time interval (ITI). On T1 (acquisition trial), subjects were placed in the apparatus containing two identical objects for 10 min (mice) or 3 min (rats) before being returned to their home cage and, following a variable ITI (2 min to 4 h), were placed back in the NOR apparatus containing a familiar (F) and a novel object (N) for 5 min (mice) or 3 min (rats) (T2, restitution trial) (*SI Appendix* Fig.S6A). The type (familiar or novel) and the position (left or right) of the two objects was counterbalanced and randomized within each experimental group during T2. Between each trial, the NOR apparatus was cleaned with water and the objects with 50 % ethanol. Exploration was defined as the animal directing the nose within 0.5 cm of the object while looking at, sniffing or touching it, excluding accidental contacts (backing into, standing on the object, etc.). The raw T2 exploration data were transformed to obtain a recognition index [Time exploring novel object / Time exploring (novel+familiar) objects] x 100. To determine NOR memory span in controls, drug-naïve animals were tested in the NOR task using different ITIs. To assess the role of D_3R in the ITI-induced NOR deficit, animals were treated with vehicle (pH-neutralized lactic acid, 10 ml/kg, s.c. or bilateral intra-PFC injection, 0.5 µl for mice and 1 µl for rats) or the D_3R antagonist S33084 (Servier, France; 0.63 mg/kg, s.c. or 2.5 µg bilateral intra-PFC injections) 30 min (s.c.) (Fig.6) or 5 min (intra-PFC) (*SI Appendix* Fig.S6A) before the acquisition trial (T1) of the NOR test.

Multiplex Single-cell RT-PCR

Patch clamp recordings of astrocytes and neurons were followed by aspiration of the cell cytoplasm into the recording electrode. cDNAs synthesis was achieved using SuperScript™ III First-Strand Synthesis System for RT-PCR (InVitrogen). Briefly, the tip of the electrode containing about 5 µl was then broken in a 0.2 ml PCR Eppendorf tube containing dNTPs and Random Hexamers (Fig.2A). This mixture was heated to 65°C for 5 min and incubated on ice for 1 min. Single-strand cDNAs were synthesized from cellular mRNA by 1 h incubation at 50°C with 5 µl of RT reaction mix containing 10X RT buffer, $MgCl_2$, DTT, Superscript III RT. Specific genes were

amplified from the resulting cDNAs by a two-step PCR. First PCR was achieved with multiplex primers targeting 6 to 8 genes of interest (including controls) on the whole RT product (10 µl) at a low annealing temperature (56 to 58°C). Second step (nested PCR) was achieved on 0.5 µl of PCR1 with a single pair of gene specific primers whose binding sites were located 3' of the primers used in the first reaction. Annealing temperature for PCR2 was 1 or 2°C higher than for PCR1. Primers used were as follow:

ACGGGAACCCCGTCGAATGC	D_1R Forward primer
CCTCAGAGGAGCCCACGGCA	D_1R Reverse primer
CTCGGGGCTCATGGTGGCTG	D_1R Nested Reverse primer
GCCATGCTGCTCACCCTCCT	D_2R Forward primer
GTGCACATCATGACATCCAGAGTGA	D_2R Reverse primer
TGCTGAATTTCCACTCACCCACCA	D_2R Nested Reverse primer
CCAGCATCCTGAACCTCTGTGCC	D_3R Forward primer
GCATCTGACAGAAACCTGGCCCT	D_3R Reverse primer
AGACCAGGACAGTCACCCCGA	D_3R Nested reverse primer
CTGTGCGCCATCAGCGTGGA	D_4R Forward primer
TCGTCCGGAGGCTGGGTGAG	D_4R Reverse primer
GCATGAGCGGACAGGGCAGG	D_4R Nested reverse primer
TCCGCTACGAGCGCAAGATGA	D_5R Forward primer
GGCCCAGCCAAACCAGACGA	D_5R Reverse primer
GGCTCCACGACTCCGGCAAC	D_5R Nested reverse primer
CTTGCAGCTCCTCCGTCGCC	Actin Forward primer
CTCCTCAGGGGCCACACGCA	Actin Reverse primer
ACCCTGGTGCCTAGGGCGG	Actin Nested Reverse primer
GAGGCCTCCTCTCACAAGTATGTGC	β3Tubulin Forward primer
GCCAGCTTGAGGGTGCGGAA	β3Tubulin Reverse Primer
GGTGAGGGCACCACGCTGAA	β3Tubulin Nested Reverse primer
ACCTGAGGCTGGAGGCGGAG	GFAP Forward primer
TGCCGCGCAAGGACTCAAGG	GFAP Reverse primer
GAGCAGCTCTGCGTTGCGGG	GFAP Nested Reverse primer

In vivo pharmacological Magnetic Resonance Imaging (phMRI)

MRI experiments were performed on 7T Pharmascan horizontal-bore magnet (16 cm bore diameter; Bruker®, Germany) with surface coils configuration, hosted by the imaging platform at Cyceron (Caen, France). MRI acquisition protocol was performed as previously described (5). Briefly, after a T2-weighted acquisition for anatomical images (TR/TEeff=2500/51.3 ms; 20 slices; resolution=0.07x0.07x0.5 mm^3), a multiple gradient echo (MGE) protocol was performed (TR=600 ms; TE=2.944, 6.517 and 10.09 ms; 14 slices; resolution=0.19x0.19x0.75 mm^3). The 120 min duration protocol of phMRI (acquisition time of 1 min per image) included 30 min acquisition for baseline, followed by injection (i.v.) of P904, a USPIO contrast agent (Guerbet Research, France). After 30 min, S33084 (0.64 mg/kg, s.c.) was administered. Then, 30 min later, D-amphetamine challenge (1 mg/kg, i.p.) was performed and MRI acquisition was continued during a further 30 min. A total of 6 mice (3 $SR^{+/+}$, 3 $SR^{-/-}$) were used for MRI experiments.

Given the structural differences between $SR^{+/+}$ and $SR^{-/-}$ mice brain (6) an anatomical brain template was generated separately for each genotype by co-registering the anatomical images and

then averaging them. Regions Of Interest (ROI; *i.e.* PFC) were manually traced on each template using Paxinos and Franklin's Mouse Brain Atlas (7). All preprocessing steps, including slice timing and motion correction, were performed using SPM5 (http://www.fil.ion.ucl.ac.uk/spm/software/spm5/). The third-echo MGE sequence was used for the analysis purposes. For each subject, the time course of the signal was extracted in every voxel inside the selected structures. A linear regression model was used to eliminate the contrast agent washout effect. The obtained approximation ($S_0(t)$) was then extended to the whole acquisition duration and subtracted from the original signal (S(t)). The cerebral blood volume changes (ΔCBV) were calculated for each image voxel inside the ROI: $\Delta CBV(t)=(\ln(S_0(t)/S(t)))/(\ln(S_{preCA}/S_0(t)))$, with S_{preCA} corresponding to the signal intensity prior to contrast agent injection. The mean signal and ΔCBV of each ROI were then calculated.

In vivo PFC microdialysis on freely moving mice

Two months old C57BL6 mice were implanted with two microdialysis probes (CMA7 model, Carnegie Medicine, Stockholm, Sweden) located in the left and right mPFC. Stereotaxic coordinates: AP +2.2, L ± 0.5, DV −1.6. Mice were allowed to recover from the surgery overnight. On the next day, the probes were continuously perfused with an aCSF (composition in mM: NaCl 148, KCl 3.5, $CaCl_2$ 1.26, NaH_2PO_4 1.0, $MgCl_2$ 1.2, $NaHCO_3$ 1.0, pH 7.4 ± 0.2) at a flow rate of 1.0 µl/min in the mPFC using CMA/100 pump (Carnegie Medicine, Stockholm, Sweden), while animals were awake and freely moving in their home cage. One hour after the start of aCSF perfusion stabilization period, four fractions were collected (one every 20 min) to measure the basal extracellular D-serine levels in the PFC. Next, the drugs, PD128907 10 µM, SKF81297 10 µM or a combination of these two drugs were dissolved in aCSF and perfused for 1 h, and three dialysates were then collected. Area under the curve (AUC) values were calculated during the sample collections as previously described (8). At the end of the experiments, localization of microdialysis probes was verified histologically according to Bert and colleagues (9). Microdialysates were rapidly frozen and kept at -80 °C until analysis of amino acid content.

Quantification of extracellular amino acids contents by chiral column liquid chromatography with tandem mass spectrometry

The D-serine (D-Ser) concentration in the microdialysis samples was measured by ultra-high performance liquid chromatography with tandem mass spectrometry (UHPLC-MS/MS). Briefly, the UHPLC-MS/MS system included a PAL autosampler (CTC Analytics, Zwingen, Switzerland) equipped with a 10 µL sample loop and operating at +6°C, an Advance UHPLC pump, and an EVOQ Elite triple quadrupole mass spectrometer (Bruker Daltonics, Billerica, MA, USA). The electrospray (ESI) source operated in a positive mode at +4500 V, the source parameters were as follows: probe gas flow 40, nebulizer gas flow 40, probe temperature +450°C, cone gas flow 20, cone temperature +200°C, the CID gas was argon set at 1.5 mTorr. The air and nitrogen were delivered by a generator Genius 3045 (Peak Scientific Instruments, Inchinnan, Scotland). The mass spectra were scanned in the MRM mode to find the optimal precursor/product ions, the collision energy and retention times for the individual amino acids and the deuterated D,L-Ser-2,3,3-d3 (C/D/N Isotopes, Pointe-Claire, Quebec, Canada) used as the internal standard. A Crownpak CR-I(+) column (150 x 3 mm, 5 µm particle size, Daicel Corp, Osaka, Japan) was used for the chiral separations of D-Ser and L-Ser. The temperature of the column oven was set to 30°C. Trifluoroacetic acid Ultra LC-MS grade (TFA), L-amino acid standard mixture (AAS18), D-Ser and all other chemicals were purchased from Sigma-Aldrich (St. Louis, MO, USA). Acetonitrile LC-MS grade (ACN) was purchased from Fisher Scientific (Göteborg, Sweden), ultrapure water was generated by a Direct-Q-3 UV water purification system (Merck Millipore, Germany). The mobile phase A was water, 0.5 % (v/v) TFA, the mobile phase B was 0.5 % TFA in ACN. The mobile phase gradient and the flow rate were as follows: 0 min, 94 % B, 400 µL/min; 2.79 min, 94 % B, 400 µL/min; 2.8 min, 50 % B, 800 µL/min; 3.3 min, 50 % B, 800 µL/min; 3.31 min, 94 % B, 400 µL/min; 4.4 min, 94 % B, 400 µL/min. Calibration standard solutions were prepared by mixing 20 µL D-Ser in the range from 1280 nM to 20 nM with AAS18 standard containing L-Ser in aCSF and pipetting 6 µL D,L-Ser-d3 (1 µM) dissolved in water. Samples were vortexed, dried and reconstituted in 20 µL of ACN, 0.5 % TFA. Concentrations of D-Ser at 20 nM and 1280 nM were estimated as the lower and the upper limits of quantification (LLOQ, ULOQ), respectively. In this

concentration range, the calibration curve was linear (R^2 = 0.999658) with RSD 8.5 %. Within-day reproducibility for lower limit of quantification (LLOQ) and upper limit of quantification (ULOQ) concentrations showed less than 15 % deviation from the nominal concentrations. Data were not corrected from *in vitro* recovery. Changes in dialysate D- and L-serine levels were determined by means of the AUC values calculated for the amount of outflow collected during the 20-60 min period treatment.

Chronic peripheral D-serine administration

D-serine solutions were freshly prepared every day in sterilized saline (+ 0.9% NaCl) and administrated to mice as previously described (10). Briefly, $SR^{+/+}$ and $SR^{-/-}$ mice were injected s.c. daily for 20 consecutive days with 300 mg/kg D-serine or vehicle for day 1 and then 150 mg/kg D-serine or vehicle. Mice were sacrificed on day 21 without receiving an injection and were used either for electrophysiology or behavioral analysis.

HPLC analysis of amino tissue content after chronic treatment

PFC tissues were obtained from the chronically treated mice used in electrophysiology and behavior experiments. Brain tissue content of D-/L-serine, D-/L-aspartate and glycine were analyzed as previously described (11, 12). Diastereoisomer derivatives obtained following precolumn derivatization with o-phthaldialdehyde (OPA)/N-acetyl-L-cysteine in 50% methanol, were resolved on a Symmetry C8 5 µm reversed-phase column (Waters, 4.6 x 250 mm), as reported in (11). Identification and quantification of D-serine, L-serine, D-aspartate, L-aspartate and glycine were based on retention times and peak areas, compared with those of standards at different concentrations. The identity of D-aspartate and D-serine peaks was further confirmed by the selective degradation catalyzed by the *Rg*DAAO M213R variant (13): the samples, added to 10 µg of the enzyme, were incubated at 30 °C for 4 hours and then derivatized. Total protein content of tissue samples was eventually determined as reported in (11).

Drugs

Stock solutions were prepared in water except for picrotoxin which was dissolved in ethanol 100 % and S33084, dissolved in lactic acid. To prevent oxidation of dopamine, 1 % of ascorbic acid was added to the 1 mM stock solution of dopamine. Furthermore, as dopamine is light sensitive, its application was performed in the dark. For experimental use, drugs were diluted at least 1/1000.

Enzymes

Recombinant wild-type and M213R variants of *Rhodotorula gracilis* D-amino acid oxidase (*Rg*DAAO; EC 1.4.3.3) were produced in *E. coli* cells and purified as previously described (13, 14). The final *Rg*DAAO preparations had a specific activity of approximately 100 and 60 U/mg protein on D-alanine and D-serine, respectively (for the wild-type) and of 11 and 4 U/mg protein on D-serine and D-aspartate (for the M213R variant) (15) : both enzymes were fully inactive on the opposite enantiomer. The effect of DA on wild-type *Rg*DAAO activity was determined by an oxygen-consumption assay on 28 mM D-alanine as a substrate. One unit corresponds to the amount of enzyme that converts 1 µmol of substrate per minute at 25 °C.

Statistical analysis

For data presenting normal distributions, statistical differences were analyzed with unpaired Student t-test or factorial and repeated measure ANOVA, as appropriate, using the Statistica 6.1 and Statview 5.0.1 softwares. Datasets for which distribution was not normal were analyzed using non-parametric Mann-Whitney U-test or Kruskal-Wallis ANOVA, as appropriate, with Statistica 6.1 or with Prism 6 software (GraphPad). α level was set at 0.05. All data are presented as means ± SEM.

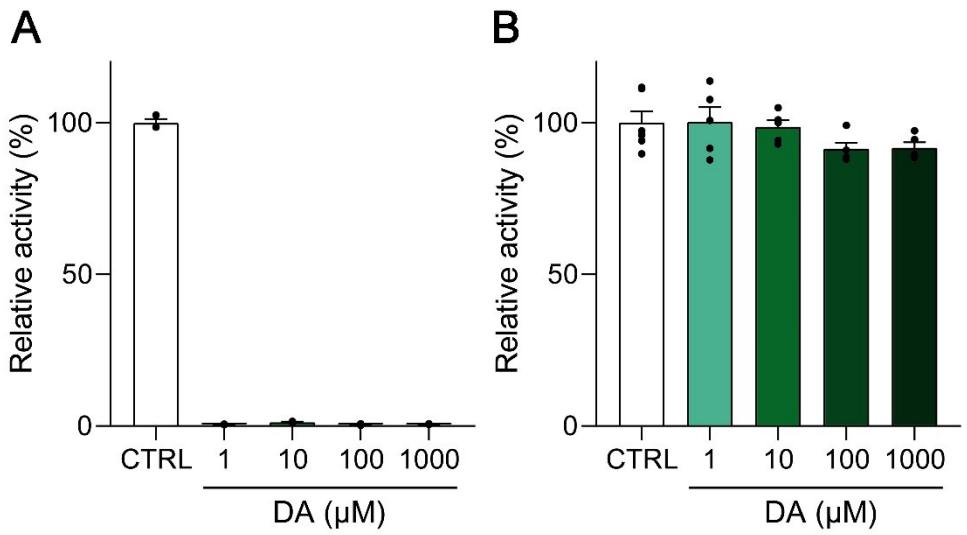

Fig. S1. Dopamine is neither a substrate nor an inhibitor for *Rg*DAAO. A, Activity of wild-type *Rg*DAAO on dopamine is virtually undetectable up to 1 mM final concentration (n=3 for each assay). This result demonstrates that dopamine is not a substrate for this flavoenzyme. B, Activity of wild-type *Rg*DAAO detected in ACSF containing 28 mM D-alanine (control conditions) is not affected by the presence of 1-1000 μM dopamine in the reaction mixtures (n=5 for each assay), thus demonstrating that it is not an inhibitor of this enzyme. In both panels, *Rg*DAAO activity is normalized to the activity on the reference substrate D-alanine (28 mM) in the absence of dopamine (CRTL, 100%).

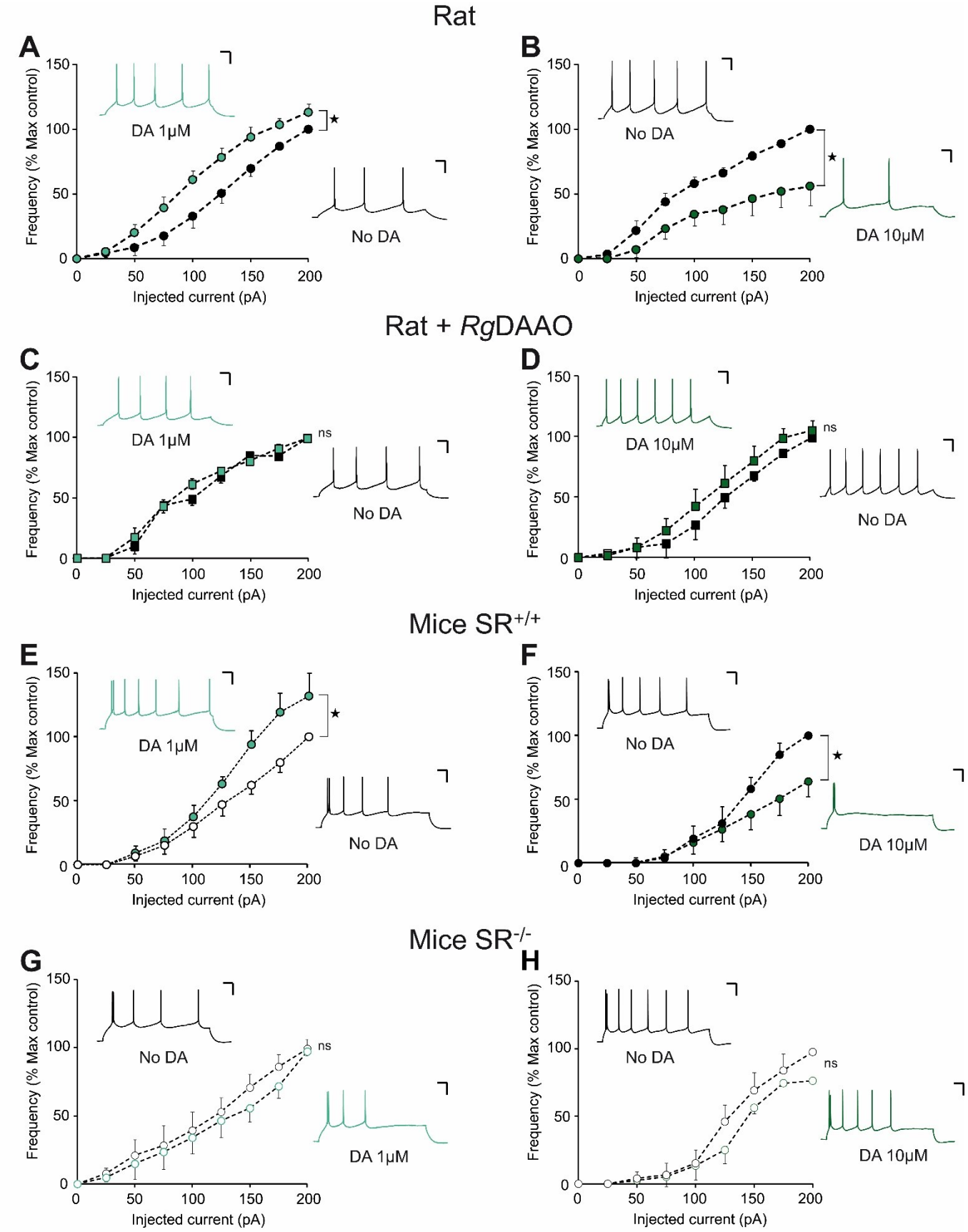

Fig. S2. D-Serine is required for DA modulation of layer 5 PFC pyramidal neurons excitability. Data are expressed as percentage of the maximal number of spike prior to treatment (% Max

control). A, Low concentration of dopamine (1 μM) upregulates neuronal excitability in rat control slices (n=7). B, High concentration of dopamine (10 μM) downregulates neuronal excitability in rat control slices (n=6). C, Depletion of D-serine with *Rg*DAAO abolishes upregulation of neuronal excitability with 1 μM dopamine (n=4) in rat PFC slices. D, Depletion of D-serine with *Rg*DAAO abolishes downregulation of neuronal excitability with 10 μM dopamine (n=5) in rat PFC slices. E, Low concentration of dopamine (1 μM) upregulates neuronal excitability in mice $SR^{+/+}$ control slices (n=8). F, High concentration of dopamine (10 μM) downregulates neuronal excitability in mice $SR^{+/+}$ control slices (n=7). G, Depletion of D-serine through genetic deletion of serine racemase abolishes upregulation of neuronal excitability with 1 μM dopamine (n=9) in $SR^{-/-}$ mice slices. H, Depletion of D-serine through genetic deletion of serine racemase abolishes downregulation of neuronal excitability with 10μM dopamine (n=7) in $SR^{-/-}$ mice slices. Scale bars: 25 pA 100 ms. * p<0.05.

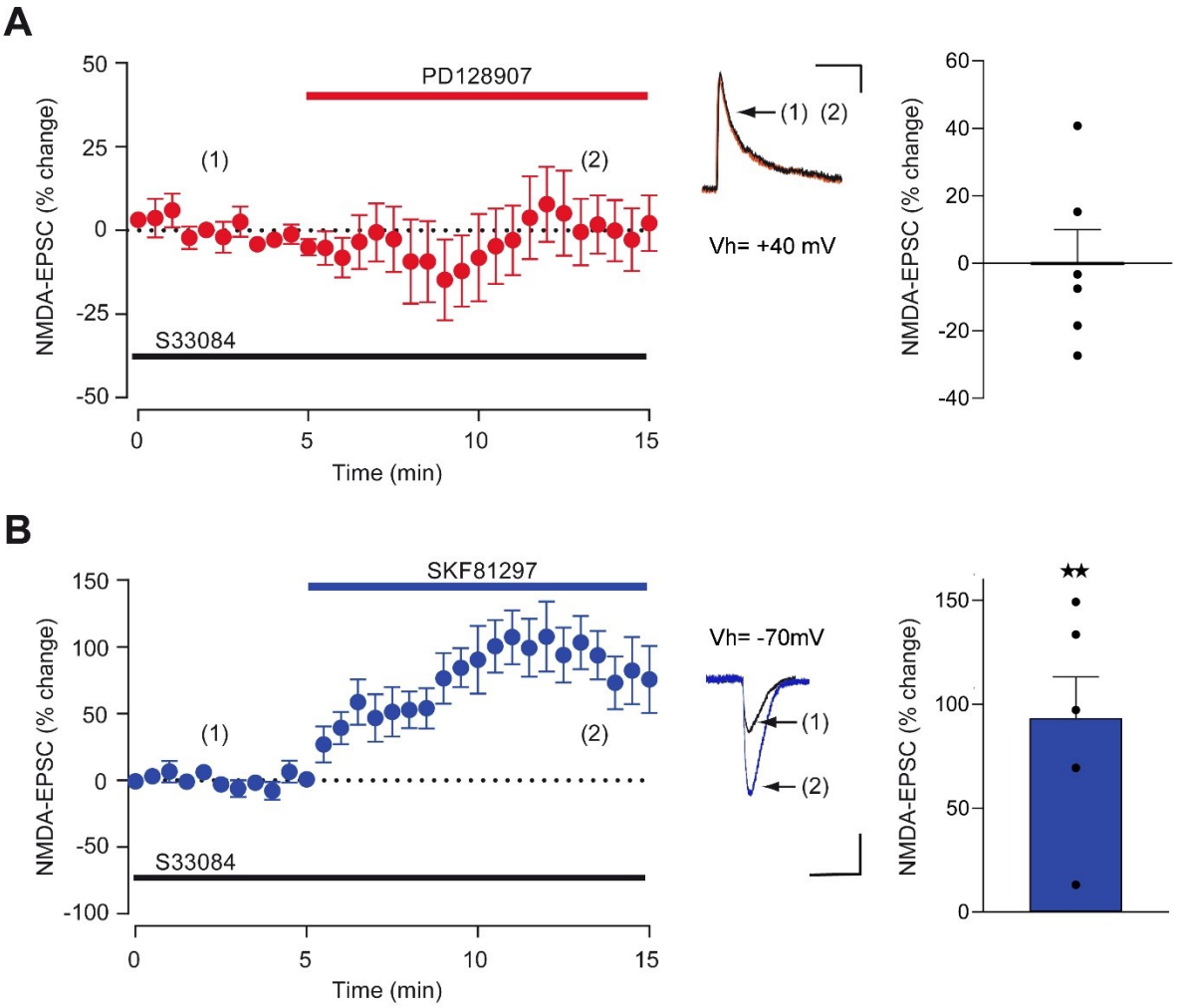

Fig. S3. D_3R specific antagonist S33084 blocks the inhibitory action of PD128907 but not the potentiating effects of SKF81297 on NMDA-EPSCs. A, Bath application of the specific D_3R antagonist S33084 (0.1 μM, Servier, France) blocks completely the effect of the D_3R agonist PD128907 (1 μM, +0.10 ± 9.88 %, n=6). Scales: 50 pA, 250 ms. Right histogram represents the average of the NMDA-EPSCs for the last 5 min. B, Bath application of S33084 does not affect the potentiating effect of the D_1R agonist SKF81297 (10 μM) on NMDA-EPSCs (+93.58 ± 17.67%, n=6). Scales: 50 pA, 100 ms. Right histogram represents the average of the NMDA-EPSCs for the last 5 min. **p<0.01.

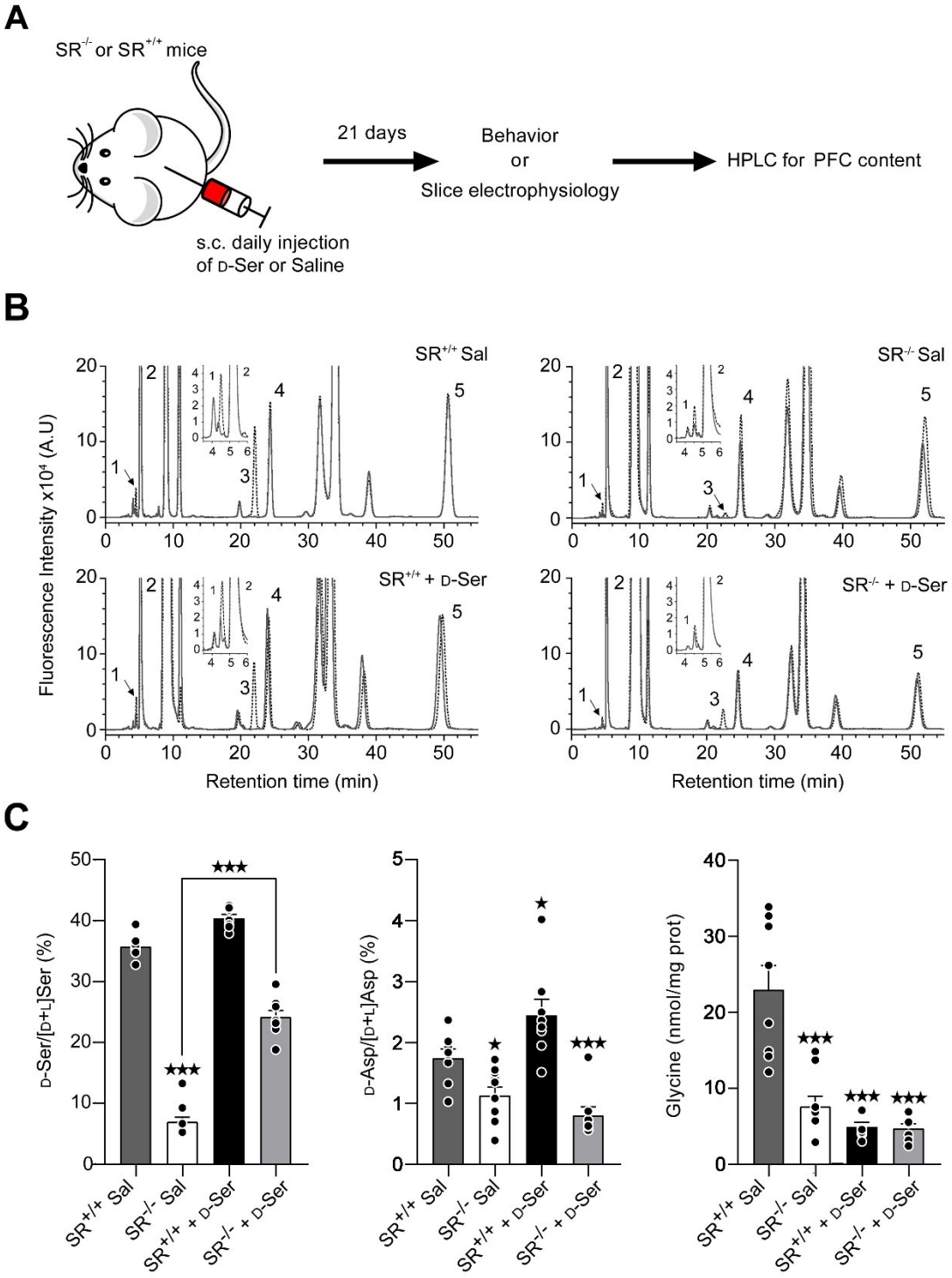

Fig. S4. HPLC analysis of PFC amino acids levels in SR$^{+/+}$ and SR$^{-/-}$ mice before and after chronic D-serine supplementation treatment. A, Diagram depicting the protocol for SR$^{+/+}$ or SR$^{-/-}$ mice treatment with D-serine or vehicle (saline) s.c injection and subsequent analyses. B, Representative HPLC chromatograms of mPFC samples from saline (Sal) and D-serine (D-Ser) treated SR$^{+/+}$ or SR$^{-/-}$ mice (dotted line). The identity of D-Ser and D-Asp peaks was verified by incubating the samples with the *Rg*DAAO M213R variant before analysis (gray line). The inset in each panel shows in detail the D-Asp peak. The peaks in the chromatograms are numbered as follows: 1, D-aspartate (D-Asp); 2, L-aspartate (L-Asp); 3, D-serine; 4, L-serine (L-Ser); 5, glycine. C, Summary bar graph depicting D-Ser and D-Asp contents (expressed as the D-Ser over total serine percentage ratio), as well as glycine content (reported as nmol/mg total protein in the tissue samples). n=8 for all samples with the exception of SR$^{-/-}$ saline for which n=10. *p<0.05, ***p<0.001.

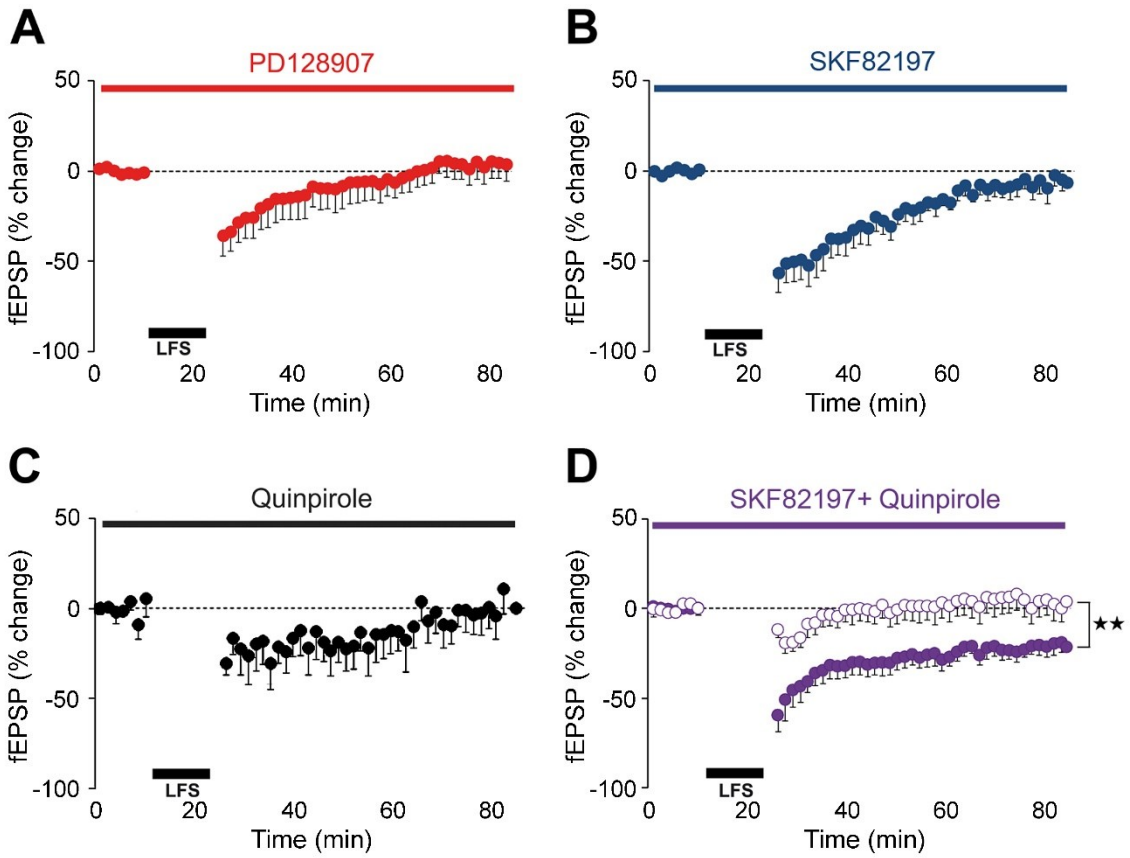

Fig. S5. Induction of LTD in the mPFC depends on the activation of both D_1-type and D_3-receptors. A, Stimulation of D_3Rs throughout the low frequency stimulation (LFS) experiment failed to produce long-term depression (LTD) (filled red circles; n=7). B, Stimulation of D_1-type receptors throughout the LFS experiment failed to produce LTD (filled blue circles; n=5). C, Stimulation of D_2-type receptors throughout the LFS experiment failed to produce LTD (filled black circles; n=5). D, Concomitant stimulation of D_1- and D_2-type receptors coupled to LFS successfully triggered LTD in control C57BL/6 (filled purple circles; n=5) but not in $D_3R^{-/-}$ mice (empty purple circles; n=5).

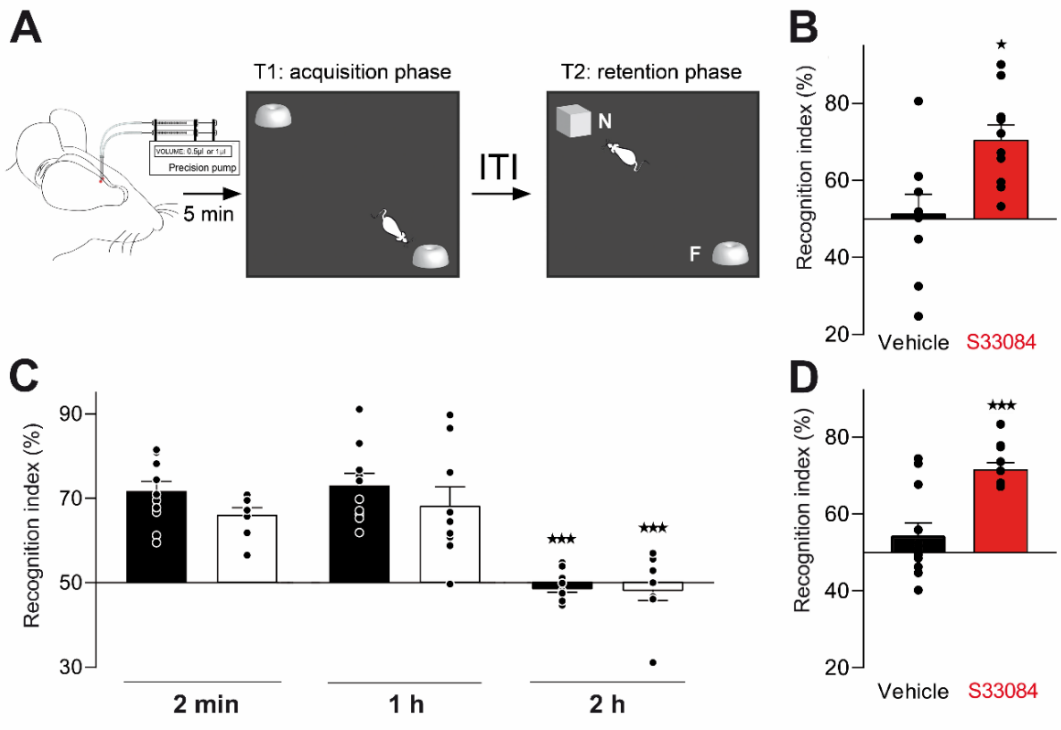

Fig. S6. Intra-PFC administration of S33084 yields pro-cognitive effects. A, Diagram showing the experimental design with intra-PFC infusion of S33084 (2.5 µg) 5 minutes before acquisition phase (T1). B, After 4h inter-trial interval (ITI), control rats injected with vehicle (n=10) showed no novel object recognition (NOR) memory, while S33084 treated rats (n=10) showed preference for the novel object. C, Untreated control $SR^{+/+}$ (n=11, black) as well as $SR^{-/-}$ mice (n=8, white) retain NOR memory up to 1h ITI. D, Intra-PFC administration of S33084 in control mice protracts NOR memory at 2h ITI (vehicle, n=12; S33084, n=11). *p<0.05, ***p<0.001.

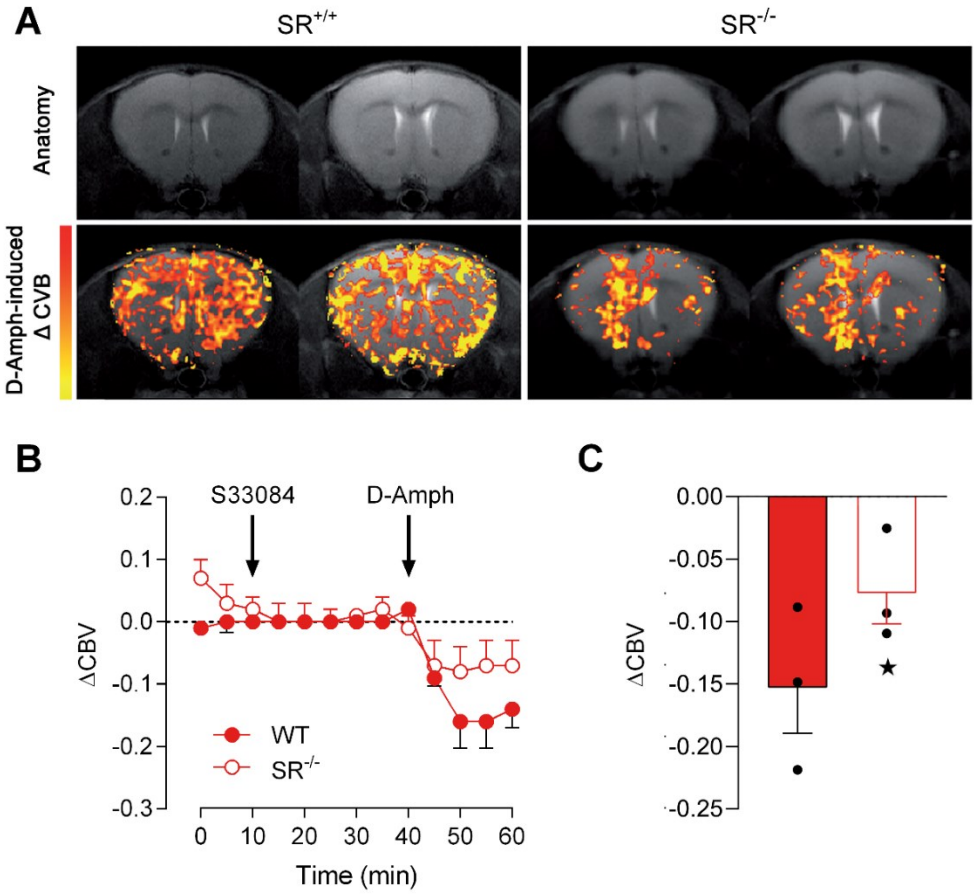

Fig. S7. Pharmacological MRI reveals that dopaminergic regulation of PFC activation is impaired in SR$^{-/-}$ mice. A, Group map of the effect of D-amphetamine (1 mg/kg, i.p.; D-Amph) after pretreatment with the D_3R antagonist S33084 (0.63 mg/kg, s.c.). The upper panels represent two 500 µm brain coronal sections used for analysis which both contain PFC. On the lower panels is superimposed in red to yellow the gradient used to indicate the magnitude of cerebral blodd volume (rCBV) variations in response to D-Amph. B, Time course showing the reducing effect of S33084 application and D-Amph injection on rCBV in SR$^{+/+}$ mice (filled circles, n=3) *vs* SR$^{-/-}$ mice (open circles, n=3) in the PFC. C, Corresponding histograms quantifying the reduction in rCBV after S33084 and D-Amph injection in control mice *vs* SR$^{-/-}$ mice in the PFC (-0.152 ± 0.034 % *vs* -0.076 ± 0.027 %, n=3). *p<0.05.

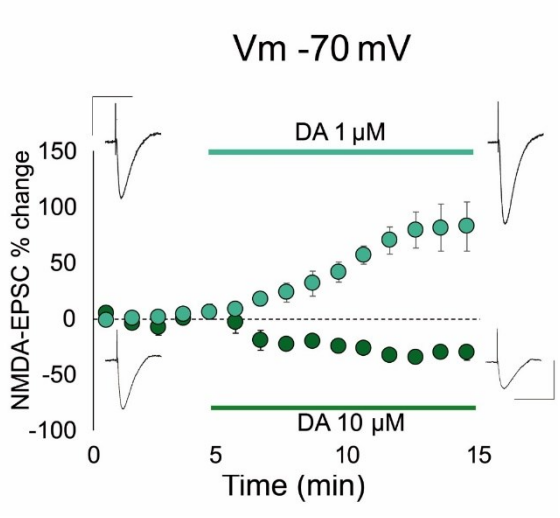

Fig. S8. Bidirectionnal modulation of NMDA-EPSCs by dopamine. Low (1µM, n=6) and high concentration (10 µM, n=5) of dopamine respectively up- and downregulates NMDA-EPSCs at resting membrane potential (Vm: -70 mV). Scale bars: 25 pA, 100 ms

	Dopamine 1 µM						Dopamine 10 µM					
	No *Rg*DAAO			*Rg*DAAO			No *Rg*DAAO			*Rg*DAAO		
	No DA	DA 1 µM	*p*	No DA	DA 1 µM	*p*	No DA	DA 10 µM	*p*	No DA	DA 10 µM	*p*
RMP (mV)	-71.16±3.25	-70.84±3.47	0.94	-69.50±1.25	-72.15±1.85	0.28	-68.12±1.57	-68.87±1.52	0.74	-68.07±2.33	-68.52±2.03	0.89
Rin (MΩ)	157.61±18.39	147.41±17.09	0.69	197.75±24.45	214.56±21.82	0.48	234.95±35.31	191.94±36.47	0.42	187.65±39.80	160.6±30.75	0.61
T0 (ms)	49.38±5.62	47.29±5.52	0.87	46.9±6.03	52.5±3.09	0.44	57.70±5.28	49.98±6.73	0.42	46.27±7.82	41.41±6.82	0.85
C (nF)	0.32±0.02	0.32±0.02	0.79	0.24±0.02	0.25±0.03	0.68	0.26±0.02	0.30±0.05	0.39	0.26±0.02	0.26±0.03	0.65

Table S1. Dopamine does not alter rat L5PyrNs membrane properties. Effect of dopamine 1 and 10 µM on resting membrane potential (RMP), input resistance (Rin), membrane time constant (T0) and capacitance (C) in the presence or absence of *Rg*DAAO in rats.

	Dopamine 1 µM						Dopamine 10 µM					
	Control mice			$SR^{-/-}$ mice			Control mice			$SR^{-/-}$ mice		
	No DA	DA 1 µM	*p*	No DA	DA 1 µM	*p*	No DA	DA 10 µM	*p*	No DA	DA 10 µM	*p*
RMP (mV)	-73.89±1.49	-73.79±1.51	0.96	-71.12±2.63	-71.47±2.63	0.92	-75.93±1.95	-76.65±1.61	0.78	-72.80±1.64	-71.83±1.72	0.69
Rin (MΩ)	174.96±32.43	206.36±44.90	0.58	164.80±29.21	190.41±20.31	0.48	149.66±15.26	157.56±15.00	0.72	138.34±16.40	142.90±15.78	0.84
T0 (ms)	33.13±5.54	34.06±3.72	0.72	29.79±2.56	30.88±2.50	0.50	25.96±4.45	26.92±3.22	0.97	24.62±2.13	24.07±2.16	0.55
C (nF)	0.19±0.01	0.19±0.02	0.89	0.15±0.04	0.17±0.01	0.76	0.17±0.01	0.17±0.02	0.86	0.18±0.02	0.17±0.01	0.86

Table S2. Dopamine does not alter mice L5PyrNs membrane properties. Effect of dopamine 1 and 10 µM on resting membrane potential (RMP), input resistance (Rin), membrane time constant (T0) and capacitance (C) in $SR^{+/+}$ and $SR^{-/-}$ mice.

SI References

1. P. Fossat, *et al.*, Glial D-serine gates NMDA receptors at excitatory synapses in prefrontal cortex. *Cereb. Cortex*, **22**, 595-606 (2012).
2. P. L. a Gabbott, T. a Warner, P. R. L. Jays, P. Salway, S. J. Busby, Prefrontal cortex in the rat: projections to subcortical autonomic, motor, and limbic centers. *J. Comp. Neurol.* **492**, 145–177 (2005).
3. N. Morisot, C. Le Moine, M. J. Millan, A. Contarino, CRF_2 receptor-deficiency reduces recognition memory deficits and vulnerability to stress induced by cocaine withdrawal. *Int. J. Neuropsychopharmacol.* **17**, 1969–1979 (2014).
4. D. J. G. Watson, *et al.*, Selective blockade of dopamine D3 receptors enhances while D2 receptor antagonism impairs social novelty discrimination and novel object recognition in rats: a key role for the prefrontal cortex. *Neuropsychopharmacology* **37**, 770–786 (2012).
5. T.-A. Perles-Barbacaru, *et al.*, Quantitative pharmacologic MRI: mapping the cerebral blood volume response to cocaine in dopamine transporter knockout mice. *Neuroimage* **55**, 622–628 (2011).
6. M. D. Puhl, *et al.*, In vivo magnetic resonance studies reveal neuroanatomical and neurochemical abnormalities in the serine racemase knockout mouse model of schizophrenia. *Neurobiol. Dis.* **73C**, 269–274 (2014).
7. G. Paxinos, C. Watson, *The Rat Brain in Stereotaxic Coordinates*, A. Press, Ed., 6th Ed. (2007).
8. T. H. Pham, *et al.*, Ketamine treatment involves medial prefrontal cortex serotonin to induce a rapid antidepressant-like activity in BALB/cJ mice. *Neuropharmacology* **112**, 198–209 (2017).
9. L. Bert, *et al.*, Rapid and precise method to locate microdialysis probe implantation in the rodent brain. *J. Neurosci. Methods*. **40**, 53–57 (2004).
10. D. T. Balu, *et al.*, Multiple risk pathways for schizophrenia converge in serine racemase knockout mice, a mouse model of NMDA receptor hypofunction. *Proc. Natl. Acad. Sci. U. S. A.* **110**, E2400-E2409 (2013).
11. D. Punzo, *et al.*, Age-related changes in D-aspartate oxidase promoter methylation control extracellular D-aspartate levels and prevent precocious cell death during brain aging. *J. Neurosci.* **36**, 3064–3078 (2016).
12. T. Nuzzo, *et al.*, Decreased free D -aspartate levels are linked to enhanced D-aspartate oxidase activity in the dorsolateral prefrontal cortex of schizophrenia patients. *npj Schizophr.* **3** (2017).
13. S. Sacchi, *et al.*, Engineering the substrate specificity of D-amino-acid oxidase. *J. Biol. Chem.* **277**, 27510–27516 (2002).
14. S. Fantinato, *et al.*, Engineering, expression and purification of a His-tagged chimeric D-amino acid oxidase from Rhodotorula gracilis. *Enzyme Microb. Technol.* **29**, 407–412 (2001).
15. L. Frattini, E. Rosini, L. Pollegioni, M. S. Pilone, Analyzing the d-amino acid content in biological samples by engineered enzymes. *J. Chromatogr. B Anal. Technol. Biomed. Life Sci.* **879**, 3235–3239 (2011).